Supporting Information

Optimization of amino acid-based poly(ester urea urethane) nanoparticles for the systemic delivery of gambogic acid for treating triple negative breast cancer

Ying Ji[a*], Juan Li[b], Shilin Xiao[c], Hiu Yee Kwan[c], Zhaoxiang Bian[c], Chih-Chang Chu[d]
[a] Institute of Textiles and Clothing, School of Fahion and Textiles, Research Institute for Intelligent Wearable Systems, Hong Kong Polytechnic University, Hunghom, Kowloon, Hong Kong SAR.
[b] CAS Key Laboratory for Biomedical Effects of Nanomaterial & Nanosafety, Institute of High Energy Physics, Chinese Academy of Sciences, Beijing 100049, PR China
[c] School of Chinese Medicine, Hong Kong Baptist University, Hong Kong SAR.
[d] Biomedical Engineering, Cornell University, Ithaca, NY, 14853, United States.

* Corresponding author. E-mail address: ying.ji@polyu.edu.hk (Y. Ji).

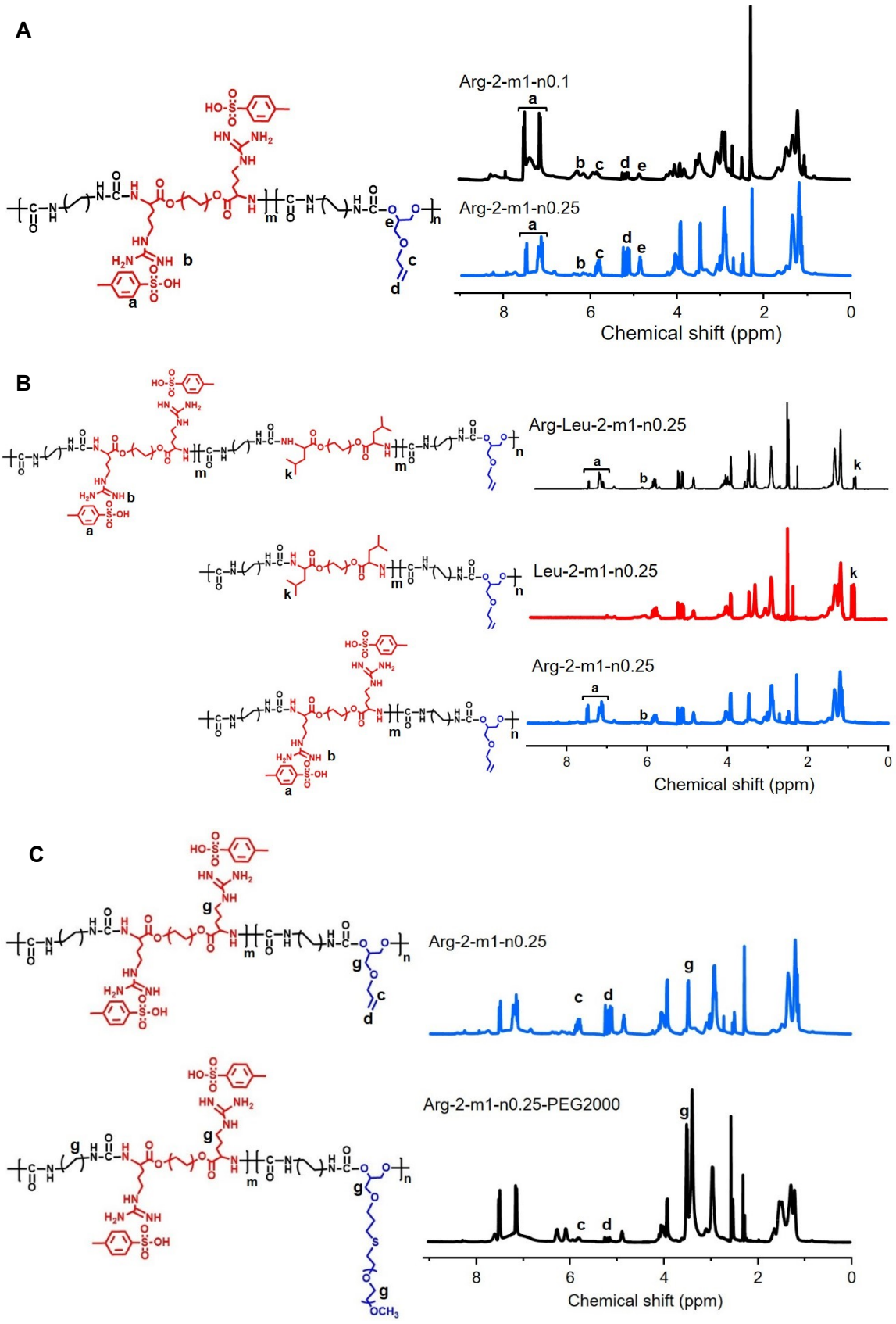

Figure S1. Representative ^{1}H-NMR spectra of AA-PEUU candidates in DMSO-*d6*. (A) ^{1}H-NMR spectra of Arg-PEUU with different m/n ratios. (B) ^{1}H -NMR spectra of single amino acid-based Arg-PEUU, Leu-PEUU or Arg-Leu-PEUU copolymer with mixed

amino acids. (C) ^{1}H-NMR spectra of Arg-PEUU before and after PEGylation.

The tunability in m/n ratio in the synthesis of AA-PEUU was demonstrated by the ^{1}H-NMR spectra of AA-PEUU in Figure S1A. Exemplified by a AA-PEUU candidate polymerized from L-arginine ethane-1,2-diester (Arg-2), HDI and GAE, with an m/n ratio of 1:0.25 (abbreviated as Arg-2-m1-n0.25), peaks representing the double bond from GAE were identified at 5.1-5.8 ppm (peaks c and d), while peaks representing the *p*-toluene sulfonic acid (TsOH) and the guanine groups from Arg-2 were identified at 6.2-7.5 ppm (peaks a and b). The area of the presentative peaks from GAE and Arg-2 correlated with the m/n ratio. The ^{1}H-NMR spectrum of Arg-2-m1-n0.25 (blue curve) was compared with another AA-PEUU candidate with a smaller m/n ratio of 1:0.1 (Arg-2-m1-n0.1, black curve) in Figure S1A. Compared to Arg-2-m1-n0.25, significantly decreased intensity of peaks c and d were observed in Arg-2-m1-n0.1, indicating the abundance of double bonds was directly correlated with the m/n ratio. The detailed peak attribution in ^{1}H-NMR spectra of Arg-2-m1-n0.25 (DMSO-*d6*) is listed below. 1.2-1.8 ppm: [-$(CH_2)_3$-C**H$_2$**-CH_2-CH_2-NH-C(O)-NH-], [-$(CH_2)_3$-CH_2-C**H$_2$**-CH_2-NH-C(O)-NH-], [-OC(O)-CH(NH-)-C**H$_2$**-CH_2-CH_2-NH(NH_2^+)-NH_2], [-OC(O)-CH(NH-)-C**H$_2$**-CH_2-CH_2-NH(NH)-NH_2]; 2.29 ppm: [**H$_3$**C-Ph-SO_3-]; 3.1-3.7 ppm: [-$(CH_2)_3$-CH_2-CH_2-C**H$_2$**-NH-C(O)-NH-], [-OC(O)-CH(R)-CH_2-CH_2-C**H$_2$**-NH(NH)-NH_2], [-NH-C(O)O-CH(R)-**CH$_2$**-O-], [-NH-C(O)O-CH(R)-C**H$_2$**-O-]; 3.9-4.2 ppm: [-O-C**H$_2$**-CH=CH_2], [-OC(O)-C**H**(R)-CH_2-CH_2-CH_2-NH(NH)-NH_2], [-C(O)O-C**H$_2$**-C**H$_2$**-O(O)C-]; 4.8 ppm: [-NH-C(O)O-C**H**(R)-CH_2-O-]; 5.2-5.3 ppm: [-O-CH_2-CH=C**H$_2$**]; 5.9 ppm [-O-CH_2-C**H**=CH_2]; 6.0-6.2 ppm: [-OC(O)-CH(R)-CH_2-CH_2-CH_2-N**H**(N**H**)-N**H$_2$**]; 7.1-7.5 ppm: [H_3C-**Ph**-SO_3-].

To investigate the tunability of amino acid type in PEUU, Arg was selected as the representative hydrophilic amino acid in AA-PEUU and Leu as the representative hydrophobic amino acid. As shown in Figure S1B, the ^{1}H-NMR spectra of Leu-2-m1-n0.25 exhibited a characteristic peak including the protons from isopropyl groups[-CH_2-CH-(C**H$_3$**)$_2$] at 0.9 ppm (peak k). Compared to the ^{1}H-NMR spectrum of Arg-2-m1-0.25, the protons from TsOH (7.1-7.5 ppm) were absent in Leu-2-m1-n0.25. This could be explained by the strong electrostatic interaction between guanine and TsOH in Arg-2, while the hydrophobic Leu-2 lacked any cationic charge to attract TsOH. The detailed peak attribution in ^{1}H-NMR spectra of Leu-2-m1-n0.25 (DMSO-*d6*) is listed below. 0.9 ppm: [-CH_2-CH-(C**H$_3$**)$_2$]; 1.2-1.8 ppm: [-$(CH_2)_3$-C**H$_2$**-CH_2-CH_2-NH-C(O)-NH-], [-$(CH_2)_3$-CH_2-C**H$_2$**-CH_2-NH-C(O)-NH-], [-OC(O)-CH(R)-C**H$_2$**-CH-$(CH_3)_2$], [-OC(O)-CH(R)-CH_2-C**H**-$(CH_3)_2$]; 3.1-3.7 ppm: [-$(CH_2)_3$-CH_2-CH_2-C**H**$_2$-NH-C(O)-NH-], [-NH-C(O)O-CH(R)-**CH$_2$**-O-], [-NH-C(O)O-CH(R)-C**H$_2$**-O-]; 3.9-4.2 ppm: [-O-C**H$_2$**-CH=CH_2], [-OC(O)-C**H**(R)-CH_2-CH-$(CH_3)_2$]], [-C(O)O-C**H$_2$**-C**H$_2$**-O(O)C-]; 4.8 ppm: [-NH-C(O)O-C**H**(R)-CH_2-O-]; 5.2-5.3 ppm: [-O-CH_2-CH=C**H$_2$**]; 5.9 ppm: [-O-CH_2-C**H**=CH_2]. In addition to single amino acid-based PEUU, AA-PEUU copolymers were developed from the polymerization of Arg-2 and Leu-2 mixture. ^{1}H-NMR spectra of Arg-2-Leu-2-m1-n0.25 copolymer in Figure S1B exhibited characteristic peaks from both Arg-2 (peaks a and b) and Leu-2 (peak k), which demonstrated the tunability of amino acid type in PEUU.

The PEGylation of AA-PEUU was demonstrated in Figure S1C. Although the

characteristic peak of ethylene glycol (C**H**$_2$-C**H**$_2$-O) at 3.6 ppm (peak g) was overlapping with the peaks from amino acid-based alkylene diester and GAE, a significant increase in the intensity of peak g was observed in PEGylated Arg-2-m1-n0.25-PEG2000 (black curve) compared to Arg-2-m1-n0.25 before PEGylation (blue curve). Meanwhile, the reduced intensity of peaks c and d from the double bond in GAE was observed, which suggested the consumption of double bonds in the reaction with cysteamine and further reacted with mPEG-SH.

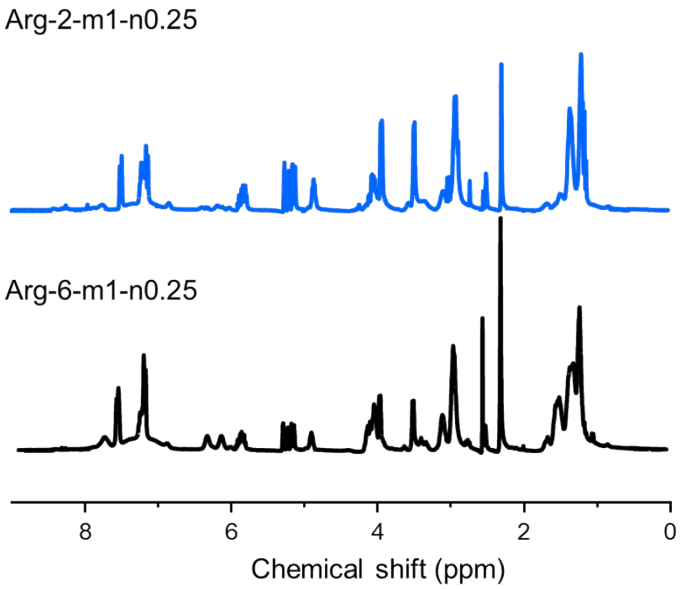

Figure S2. ^{1}H-NMR spectra of Arg-PEUU candidates with different hydrocarbons. Arg-2-m1-n0.25 was synthesized from L-arginine ethane-1,2-diester (Arg-2) and Arg-6-m1-n0.25 was synthesized from L-arginine hexane-1,6-diester (Arg-6). Due to the overlapping of the hydrocarbon peaks in the chemical shift ranging from 1.2 to 1.8 ppm, the peak attribution of Arg-6-m1-n0.25 was identical to Arg-2-m1-n0.25.

(DMSO-*d6*, ppm, δ) 1.2 to 1.8: [-$(CH_2)_3$-C**H**$_2$-CH_2-CH_2-NH-C(O)-NH-], [-$(CH_2)_3$-CH_2-C**H**$_2$-CH_2-NH-C(O)-NH-], [-OC(O)-CH(NH-)-C**H**$_2$-CH_2-CH_2-NH(NH_2^+)-NH_2], [-OC(O)-CH(NH-)-C**H**$_2$-CH_2-CH_2-NH(NH)-NH_2]; 2.29: [**H**$_3$C-Ph-SO_3-]; 3.1 to 3.7: [-$(CH_2)_3$-CH_2-CH_2-C**H**$_2$-NH-C(O)-NH-], [-OC(O)-CH(R)-CH_2-CH_2-C**H**$_2$-NH(NH)-NH_2], [-NH-C(O)O-CH(R)-**CH**$_2$-O-], [-NH-C(O)O-CH(R)-C**H**$_2$-O-]; 3.9 to 4.2: [-O-C**H**$_2$-CH=CH_2], [-OC(O)-C**H**(R)-CH_2-CH_2-CH_2-NH(NH)-NH_2], [-C(O)O-C**H**$_2$-C**H**$_2$-O(O)C-]; 4.8: [-NH-C(O)O-C**H**(R)-CH_2-O-]; 5.2 to 5.3: [-O-CH_2-CH=C**H**$_2$]; 5.9 [-O-CH_2-C**H**=CH_2]; 6.0 to 6.2: [-OC(O)-CH(R)-CH_2-CH_2-CH_2-N**H**(N**H**)-N**H**$_2$]; 7.1 to 7.5: [H_3C-**Ph**-SO_3-].

Table S1. Summary of the AA-PEUU candidates in this study.

AA-PEUU abbreviations	Amino acid	Hydrocarbons	m/n	PEG	DLS diameter (PDI)	Zeta potential
Arg-2-m1-n0	Arg	$(-CH_2-)_2$	1:0	N.A.	No NP formed	
Arg-2-m1-n0.1-PEG2000	Arg	$(-CH_2-)_2$	1:0.1	2000 Da	205.9±16.8 nm (0.24)	5.2±1.1 mV
Arg-2-m1-n0.25-PEG2000	Arg	$(-CH_2-)_2$	1:0.25	2000 Da	102.5±12.9 nm (0.19)	-8.3±2.9 mV
Leu-2-m1-n0	Leu	$(-CH_2-)_2$	1:0	N.A.	No NP formed	
Leu-2-m1-n0.1-PEG2000	Leu	$(-CH_2-)_2$	1:0.1	2000 Da	246.5±12.5 nm (0.23)	-25.6±5.2 mV
Leu-2-m1-n0.25-PEG2000	Leu	$(-CH_2-)_2$	1:0.25	2000 Da	107.9±7.5 nm (0.17)	-23.2±7.1 mV
Arg-Leu-2-m1-n0	50% Arg + 50% Leu	$(-CH_2-)_2$	1:0	N.A.	286.2±20.5 nm (0.40)	22.5±6.2 mV
Arg-Leu-2-m1-n0.1-PEG2000	50% Arg + 50% Leu	$(-CH_2-)_2$	1:0.1	2000 Da	93.2±15.6 nm (0.36)	7.2±3.9 mV
Arg-Leu-2-m1-n0.25-PEG2000	50% Arg + 50% Leu	$(-CH_2-)_2$	1:0.25	2000 Da	105.9±20.5 nm (0.38)	-2.4±0.5 mV
Arg-6-m1-n0.25-PEG2000	Arg	$(-CH_2-)_6$	1:0.25	2000 Da	119.2±10.5 nm (0.24)	-9.5±4.1 mV
Leu-6-m1-n0.25-PEG2000	Leu	$(-CH_2-)_6$	1:0.25	2000 Da	120.4±12.2 nm (0.25)	-26.5±5.2 mV
Arg-2-m1-n0.25-PEG550	Arg	$(-CH_2-)_2$	1:0.25	550 Da	98.2±7.5 nm (0.21)	4.9±1.2 mV
Arg-2-m1-n0.25-PEG5000	Arg	$(-CH_2-)_2$	1:0.25	5000 Da	113.8±8.6 (0.18)	-9.8±3.1 mV

Table S2. Theoretical vs. detected concentration of PEG in Arg-PEUU polymers with different m/n ratios.

	Arg-2-m1-n0.1-PEG2000	Arg-2-m1-n0.25-PEG2000	Arg-2-m1-n0.4-PEG2000
Theoretical PEG content (wt%)	26.8%	49.6%	69.5%
Detected PEG content (wt%)	19.2±1.5%	32.3±5.1%	34.5±8.5%

Table S3. Theoretical vs. detected concentration of PEG in Arg-PEUU polymers with different PEG molecular weights.

	Arg-2-m1-n0.25-PEG550	Arg-2-m1-n0.25-PEG2000	Arg-2-m1-n0.25-PEG5000
Theoretical PEG content (wt%)	21.3%	49.6%	71.2%
Detected PEG content (wt%)	18.3±3.6%	32.3±5.1%	36.2±11.6%

The theoretical PEG content referred to the weight percentage of PEG in the whole PEUU chain, when assuming all the GAE moieties were grafted with PEG. The detected PEG content referred to the weight percentage of PEG detected via fluorescent spectroscopy when PEUUs were conjugated with Rhodamine-labelled mPEG-SH (Rho-PEG-SH). The Arg-PEUU polymers were conjugated with Rho-PEG-SH with different molecular weights via the same synthetic procedures as described in section 2.2 (main text). The calibration curve of Rho-PEG-SH was established by the detection of the fluorescent emission curve of free Rho-PEG-SH solutions with various concentrations when excited at 561 nm on an Agilent G9800AA Cary Eclipse fluorescence spectrophotometer. The pre-weighed Arg-PEUU polymers were dissolved in DMF and the fluorescence intensity was compared with the standard calibration curve to determine the PEG concentration.

The results in **Table S2** and **Table S3** suggested that the content of PEG was impacted by the m/n ratios and the molecular weight of PEG. At low to medium m/n ratios (Arg-2-m1-n0.1-PEG2000 and Arg-2-m1-n0.25-PEG2000), the deviation between the calculated and the detected PEG concentration was not significant and the PEG content increased with the m/n ratio. However, in the case of Arg-2-m1-n0.4-PEG2000, the content of PEG in Arg-PEUU did not further increase. A potential threshold of PEG that could be grafted onto Arg-PEUU existed, which could be explained by the steric hindrance of the pendant PEG chains.

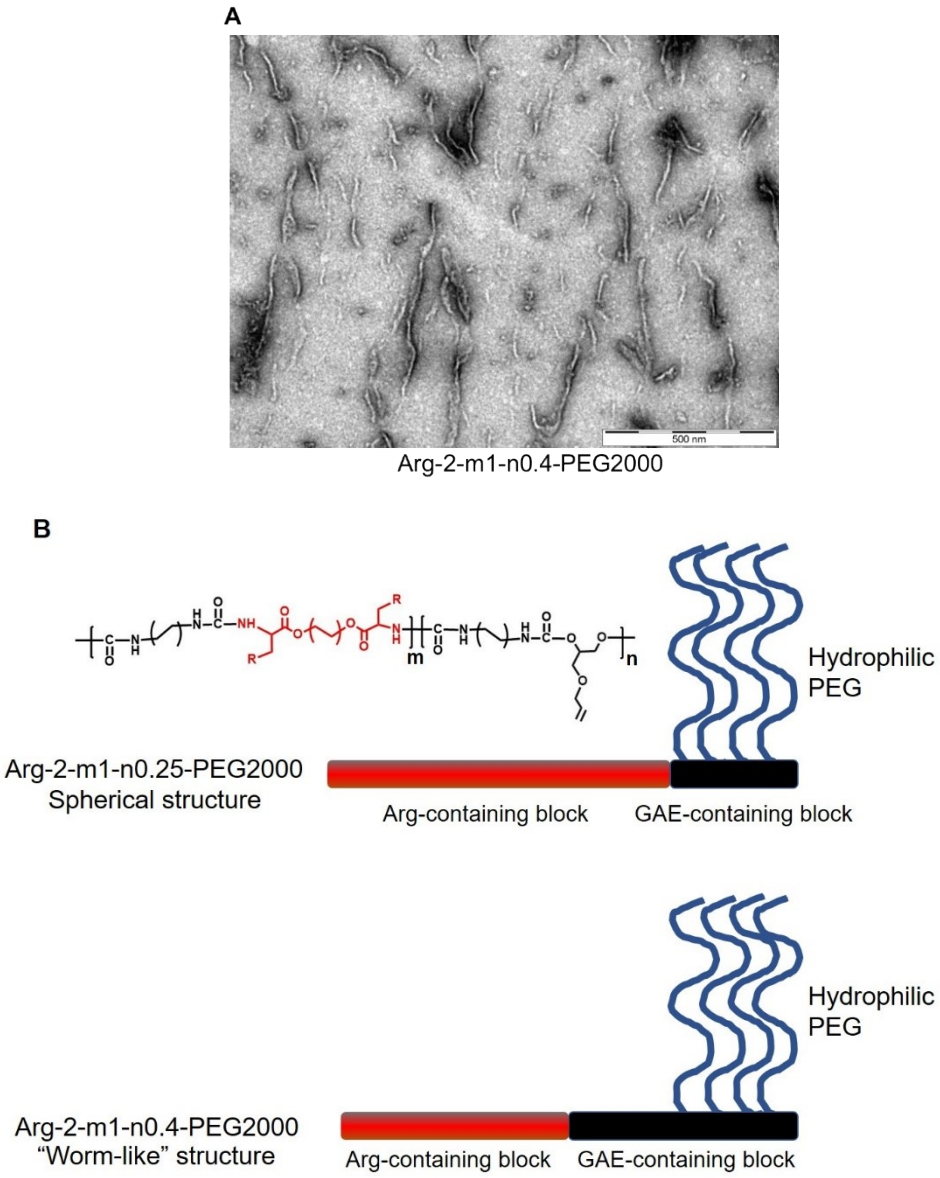

Figure S3. (A) TEM morphology of Arg-PEUU candidate (Arg-2-m1-n0.4) with an m/n ratio of 1:0.4. When the m/n ratio increased to 1:0.4, the as-formed nanostructure transformed from a spherical morphology into a worm-like morphology. Scale bar=500 nm. The cartoon of Arg-2-m1-n0.25-PEG2000 and Arg-2-m1-n0.4-PEG2000 to compare the hydrophilic/hydrophobic segments. (B) The cartoon of Arg-2-m1-n0.25-PEG2000 and Arg-2-m1-n0.4-PEG2000 to compare the hydrophilic/hydrophobic segments.

The results in **Table S3** suggested that the content of PEG was impacted by the molecular weight of PEG. PEG with greater molecular weight could also result in great steric hindrance, which could explain the significant difference between the calculated vs. detected PEG5000 in Arg-2-m1-n0.25-PEG5000. The PEGylation ratio of Arg-2-m1-n0.4-PEG2000 was almost equivalent to Arg-2-m1-n0.25-PEG2000. **Figure S3B** indicated the hydrophobic/hydrophilic balance in Arg-PEUUs. In Arg-2-m1-n0.4-

PEG2000, the un-consumed GAE block (black in color) was hydrophobic compared to the Arg-containing block (red in color), therefore, more hydrophobic segments existed in Arg-2-m1-n0.4-PEG2000. The dependency of morphology on the hydrophobicity/hydrophilicity ratio was summarized in previous studies.[1,2] Spherical micelles were favored when more hydrophilic segments existed (with a packing parameter $p \leq 1/3$), when the hydrophobic components increased ($1/3 \leq p \leq 1/2$), cylindrical or wormlike micelles were formed. Therefore, the worm-like structure of Arg-2-m1-n0.4-PEG2000 could be related to the increased hydrophobic segments compared to Arg-2-m1-n0.25-PEG2000.

The rationale for the selection of amino acids, hydrocarbons and PEG in this study

Amino acid. Firstly, we aimed to select one representative hydrophilic amino acid and one hydrophobic amino acid to develop the representative AA-PEUU candidates and explore the trend of amino acid type on the self-assembly of PEUU polymers driven by hydrophobic/hydrophilic segments. Secondly, arginine has been previously reported[3] to form complexes with GA via guanidyl groups to promote the *in vivo* delivery performance. Therefore, arginine was selected as the representative hydrophilic amino acid to develop AA-PEUU candidates. Thirdly, leucine-based PEUU was selected as the representative hydrophobic amino acid-based PEUU to explore the hydrophobicity/hydrophilicity impact of the amino acid residue in nanoparticle formation and GA loading.

Hydrocarbon. The selection of hydrocarbon impacted the hydrophilic/hydrophobic balance of AA-PEUU and further impacted the formation of nanoparticles. In our preliminary studies, when 1,8-octanediol $(-CH_2-)_8$ was selected for the synthesis of Arg-PEUU, at an equivalent m/n ratio (Arg-8-m1-n0.25-PEG2000), both worm-like and spherical nanostructures were detected in the TEM characterization, suggesting the Arg-8-m1-n0.25-PEG2000 contained more hydrophobic segments. In addition, previous study[4,5] of our group suggested that the introduction of long hydrocarbons such as $(-CH_2-)_8$ could dilute the concentration of amino acids, which could reduce the enzymatic biodegradation rate of the polymers and further reduce the drug release rate. Therefore, shorter hydrocarbons $(-CH_2-)_2$ and $(-CH_2-)_6$ were selected for this study.

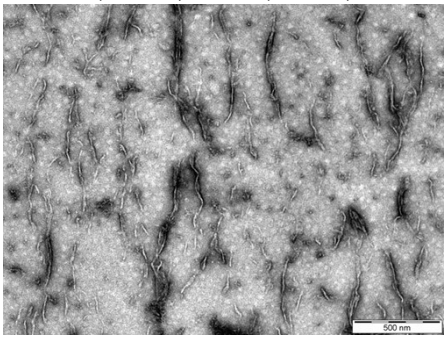

Figure S4. TEM characterization of Arg-8-m1-n0.25-PEG2000 synthesized from 1,8-octanediol.

Molecular weights of PEG. The selection of PEG was determined by a balance between sufficient stealthy performance and ease of the grafting reaction. Longer PEG

usually resulted in greater steric hindrance, which could introduce additional challenges to the grafting of PEG onto PEUU. Table S3 showed the comparison of the quantification of grafted PEG vs. the theoretical PEG concentration. PEG5000 resulted in a great deviation between the theoretical and the detected PEG content, suggesting that a significant fraction of GAE blocks was not conjugated with PEG5000. The impact of PEG molecular weight on the grafted content could be explained by the increasing steric hindrance of long PEG chains could add difficulties for the grafting. Therefore, PEG with a molecular weight greater than 5000 Da was not selected for the study. Furthermore, PEG with a shorter molecular weight could not provide enough surface hydration of nanoparticles for long circulation *in vivo*.[6] In this regard, PEG with molecular weights of 550 Da, 2000 Da and 5000 Da were selected.

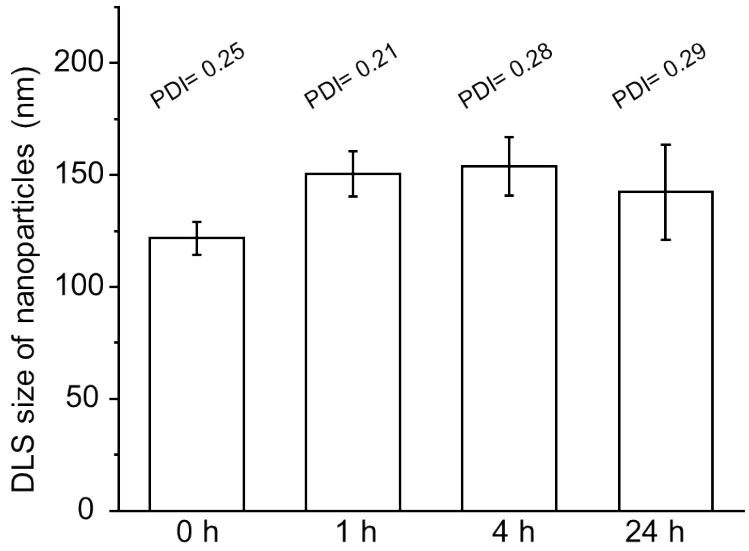

Figure S5. Stability of GA-loaded Arg-2-m1-n0.25-PEG2000 nanoparticles. DLS size detection of GA-loaded nanoparticles after incubation in 10% FBS in PBS for 1 h, 4 h, or 24 h. After incubation for up to 24 h, the nanoparticles become slightly greater in DLS diameter but no significant nanoparticle aggregation or sharp changes of PDI were detected. The stability of Arg-PEUU-NP-GA in the physiological condition could be related to the hydrophobic interaction and π–π interaction between GA and PEUU polymers. Meanwhile, the potential formation of electrostatic complexation between the arginine residue and GA could further enhance the stability of Arg-PEUU-NP-GA.

A

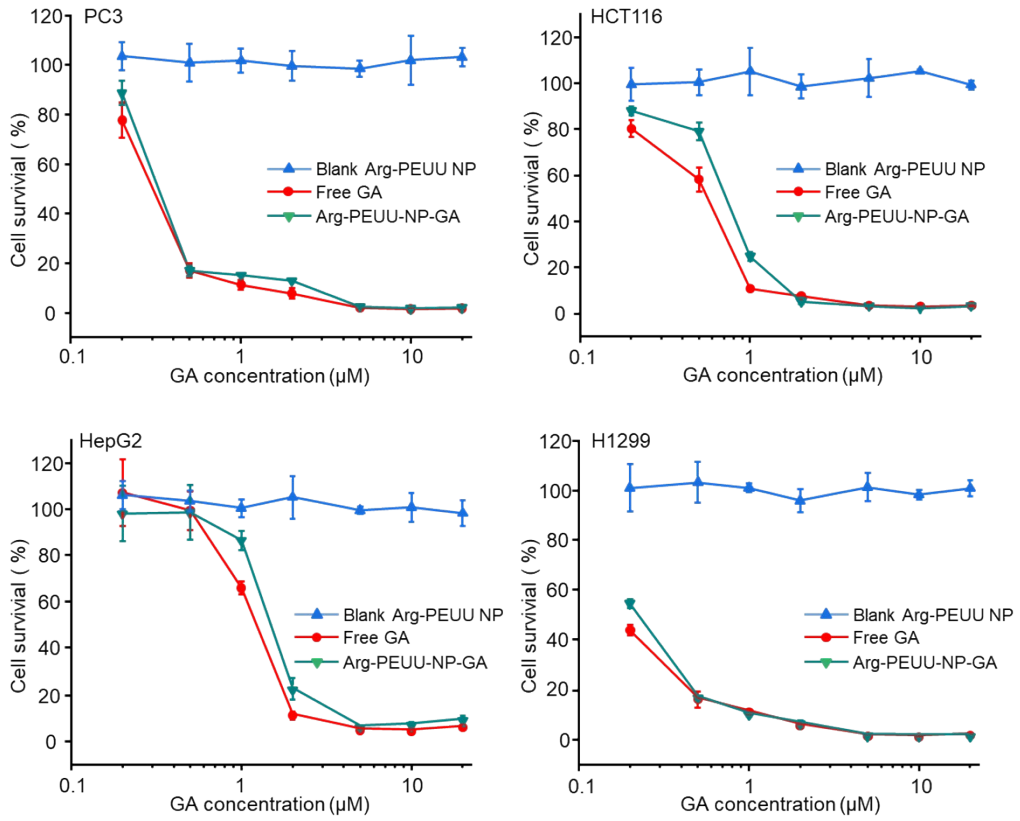

B

IC50	Free GA	Arg-PEUU-NP-GA
PC3	0.29 μM	0.33 μM
HCT116	0.58 μM	0.72 μM
HepG2	1.28 μM	1.65 μM
H1299	<0.2 μM	0.24 μM

Figure S6. Inhibitory effect of free GA, GA-loaded Arg-PEUU-NP (Arg-PEUU-NP-GA) on different cancer cell lines. PC3 prostate cancer cells, HCT116 colon cancer cells, HepG2 liver cancer cells or H1299 non-small lung carcinoma cells were treated with free GA or Arg-PEUU-NP-GA at equivalent GA concentrations for 48 h. (A) The viability of cells was detected by MTS assay (n=3) and normalized to saline-treated controls. Cells treated with blank Arg-PEUU NP were also tested. The IC50 in each cell line was calculated as follows. (B) The half-maximal inhibitory concentration (IC50) was determined. The results suggested that Arg-PEUU-NP-GA demonstrated competitively inhibitory effect as compared to free GA. The sensitivity of GA (both free and loaded) varied on different cell lines. Among all the cancer cell lines investigated in this study, MDA-MB-231, HepG2 and HCT116 cells were mildly sensitive to GA, while PC3 and H1299 cells were very sensitive to GA. The results also indicated the potential of GA in treating different types of tumors.

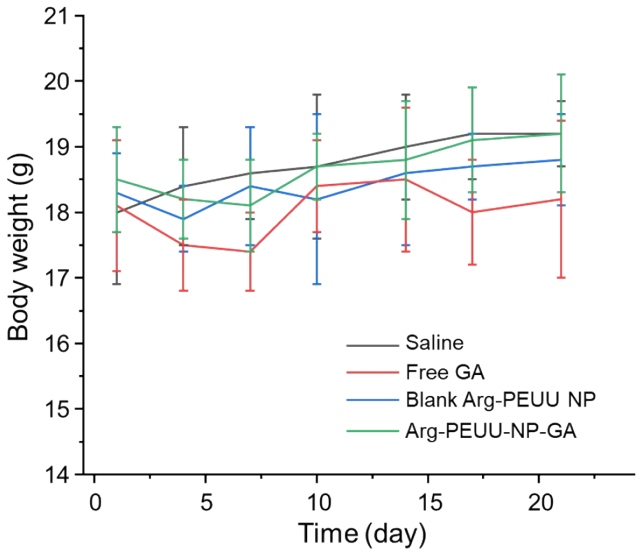

Figure S7. Bodyweight monitoring of MDA-MB-231 tumor-bearing mice receiving intravenous injection of saline, free GA, blank Arg-PEUU NP, Arg-PEUU-NP-GA, with an equivalent GA dose of 4 mg/kg/injection (n=4). Intravenous injections were performed on days 1, 4, 7, 10 and 14. The tumor-bearing mice were weighed on days 1, 4, 7, 10, 14, 17 and 21. No significant loss of body weight was observed in the 4 tested groups.

References:

1. Israelachvili, Jacob N., D. John Mitchell, and Barry W. Ninham. "Theory of self-assembly of hydrocarbon amphiphiles into micelles and bilayers." Journal of the Chemical Society, Faraday Transactions 2: Molecular and Chemical Physics 72 (1976): 1525-1568.

2. Karayianni, Maria, and Stergios Pispas. "Block copolymer solution self-assembly: Recent advances, emerging trends, and applications." Journal of Polymer Science 59.17 (2021): 1874-1898.

3. Yu, Fan, Fuguang, Jiang, Xinhui, Tang, and Bochu, Wang. "N-octyl-N-arginine-chitosan micelles for gambogic acid intravenous delivery: characterization, cell uptake, pharmacokinetics, and biodistribution." Drug Development and Industrial Pharmacy 44.4 (2018): 615-623.

4. Guo, Kai, and C. C. Chu. "Synthesis, characterization, and biodegradation of copolymers of unsaturated and saturated poly (ester amide)s." Journal of Polymer Science Part A: Polymer Chemistry 45.9 (2007): 1595-1606.

5. Wu, Jun, and C. C. Chu. "Water insoluble cationic poly (ester amide) s: synthesis, characterization and applications." Journal of Materials Chemistry B 1.3 (2013): 353-360.

6. Jokerst, Jesse V., Lobovkina, Tatsiana, Zare, Richard and Gambhir, Sanjiv. "Nanoparticle PEGylation for imaging and therapy." Nanomedicine 6.4 (2011): 715-728.